A High-Cholesterol Diet Exacerbates Liver Fibrosis in Mice via Accumulation of Free Cholesterol in Hepatic Stellate Cells

TOSHIAKI TERATANI,* KENGO TOMITA,*,‡ TAKAHIRO SUZUKI,* TETSUYA OSHIKAWA,* HIROKAZU YOKOYAMA,§ KATSUYOSHI SHIMAMURA,* SUSUMU TOMINAGA,‖ SADAYUKI HIROI,‖ RIE IRIE,¶ YOSHIKIYO OKADA,‡ CHIE KURIHARA,‡ HIROTOSHI EBINUMA,* HIDETSUGU SAITO,# RYOTA HOKARI,‡ KAZUO SUGIYAMA,* TAKANORI KANAI,* SOICHIRO MIURA,‡ and TOSHIFUMI HIBI*

*Division of Gastroenterology and Hepatology, Department of Internal Medicine, §Health Center, Keio University School of Medicine, Tokyo, Japan; ‡Division of Gastroenterology and Hepatology, Department of Internal Medicine, ‖Department of Pathology and Laboratory Medicine, National Defense Medical College, Saitama, Japan; ¶Department of Pathology, Kawasaki Municipal Hospital, Kanagawa, Japan; #Graduate School of Pharmaceutical Sciences, Keio University Faculty of Pharmacy, Tokyo, Japan

See editorial on page 8.

BACKGROUND & AIMS: Some studies have indicated that dietary cholesterol has a role in the progression of liver fibrosis. We investigated the mechanisms by which dietary cholesterol might contribute to hepatic fibrogenesis. **METHODS:** C57BL/6 mice were fed a high-cholesterol diet or a control diet for 4 weeks; liver fibrosis then was induced by bile-duct ligation or carbon tetrachloride administration. Hepatic stellate cells (HSCs) were isolated from mice fed high-cholesterol diets or from Niemann-Pick type C1-deficient mice, which accumulate intracellular free cholesterol. **RESULTS:** After bile-duct ligation or carbon tetrachloride administration, mice fed high-cholesterol diets had significant increases in liver fibrosis and activation of HSCs compared with mice fed control diets. There were no significant differences in the degree of hepatocellular injury or liver inflammation, including hepatocyte apoptosis or Kupffer cell activation, between mice fed high-cholesterol or control diets. Levels of free cholesterol were much higher in HSCs from mice fed high-cholesterol diets than those fed control diets. In cultured HSCs, accumulation of free cholesterol in HSCs increased levels of Toll-like receptor 4 (TLR4), leading to down-regulation of bone morphogenetic protein and activin membrane-bound inhibitor (a pseudoreceptor for transforming growth factor [TGF]β); the HSCs became sensitized to TGFβ-induced activation. Liver fibrosis was not aggravated by the high-cholesterol diet in C3H/HeJ mice, which express a mutant form of TLR4; HSCs that express mutant TLR4 were not activated by accumulation of free cholesterol. **CONCLUSIONS: Dietary cholesterol aggravates liver fibrosis because free cholesterol accumulates in HSCs, leading to increased TLR4 signaling, down-regulation of bone morphogenetic protein and activin membrane-bound inhibitor, and sensitization of HSC to TGFβ. This pathway might be targeted by antifibrotic therapies.**

Keywords: Liver Disease; Mouse Model; Dyslipidemia; Lipopolysaccharide.

Liver fibrosis, a condition that indicates the progression of liver diseases, may progress to cirrhosis or hepatocellular carcinoma.[1] For this reason, it is important to thoroughly determine the pathologic mechanisms associated with this disorder.

Dietary factors are likely to be important determinants of liver fibrosis development. Data derived from 9221 participants in the first National Health and Nutrition Examination Survey in the United States showed that higher dietary consumption of cholesterol was associated with a higher risk of cirrhosis or liver cancer in both unadjusted and adjusted analyses.[2]

Several studies also have reported that statins and ezetimibe (cholesterol-lowering agents) improve liver fibrosis in patients with hypercholesterolemia.[3,4] In recent laboratory studies, rodents or rabbits developed liver fibrosis after long-term consumption of a high-cholesterol (HC) diet containing cholic acid (atherogenic diet) or a high-fat HC diet.[5,6] However, experiments using such diets are not suitable for explaining the exact role of cholesterol in the development of liver fibrosis because cholic acid and free fatty acids induce hepatic fibrosis genes,[7] hepatocyte apoptosis, and liver inflammation.[8] Although these studies are part of a growing accumulation of evidence showing the key role of cholesterol in the development and progression of liver fibrosis, the exact role of cholesterol in the mechanisms underlying liver fibrosis remains to be explored.

To clarify the precise impact of cholesterol in the pathophysiology of liver fibrosis, we therefore used experimental models involving administration of HC diets not containing cholic acid or an excessive amount of fatty

Abbreviations used in this paper: AcLDL, acetyl low-density lipoprotein; ALT, alanine aminotransferase; Bambi, BMP and activin membrane-bound inhibitor; BDL, bile duct ligation; CCl_4, carbon tetrachloride; CE, cholesterol ester; compound 58035, acyl-CoA:cholesterol acyltransferase inhibitor 58035; FC, free cholesterol; HC, high cholesterol; HSCs, hepatic stellate cells; KO, knock-out; LPS, lipopolysaccharide; mRNA, messenger RNA; NPC1, Niemann-Pick type C1; αSMA, α-smooth muscle actin; TC, total cholesterol; TG, triglyceride; TGFβ, transforming growth factor β; TLR4, Toll-like receptor 4; TNFα, tumor necrosis factor-α; WT, wild-type.

0016-5085/$36.00
doi:10.1053/j.gastro.2011.09.049

acids to mice in which liver fibrosis was induced by bile duct ligation (BDL) or carbon tetrachloride (CCl_4) intoxication. Hepatic stellate cells (HSCs), the main producers of extracellular matrix in the fibrotic liver, play a key role in liver fibrosis, although liver fibrosis is strongly associated with some elements of liver injury, including hepatocyte death and Kupffer cell activation.[1] Our results show that consumption of an HC diet caused accumulation of free cholesterol in HSCs, which in turn significantly suppressed the expression of the transforming growth factor-β (TGFβ) pseudoreceptor bone morphogenetic protein and activin membrane-bound inhibitor (Bambi) through enhancement of Toll-like receptor 4 (TLR4) signaling, leading to aggravation of liver fibrosis.

Materials and Methods

Please refer to the Supplementary Materials and Methods section for more detailed descriptions.

Animal Model

Male 8-week-old wild-type (WT) C57BL/6, C3H/HeN, or C3H/HeJ mice were fed an HC (1% wt/wt) diet (TD 92181) or a corresponding control diet (Teklad no. 7001; Harlan Teklad, Madison, WI) for 4 weeks, and then either underwent BDL for 3 weeks, or were given CCl_4 at a dose of 5 μL (10% CCl_4 in corn oil)/g body weight, by intraperitoneal injection twice a week for 4 weeks.

Statistical Analysis

All data are expressed as the means ± standard errors of the means. Statistical analyses were performed using the unpaired Student *t* test or 1-way analysis of variance ($P < .05$ was considered significant).

Results

HC Diet Significantly Accelerated BDL- and CCl_4-Induced Liver Fibrosis

C57BL/6 mice were administered either an HC or control diet for 4 weeks and then divided into 2 groups: one group underwent BDL for 3 weeks and the other group received sham treatment. In a similar but separate experiment, mice were fed an HC or control diet for 4 weeks and then divided into 2 groups: one for 4-week treatment with CCl_4 and the other for treatment with corn oil.

The HC diet did not increase mean body or liver weight vs control (Supplementary Table 1). Although the HC diet significantly increased the serum concentration of total cholesterol (TC), no change was noted in serum triglyceride (TG) and glucose levels (Supplementary Table 1). In addition, the HC diet alone was not sufficient to cause hepatic steatosis or liver fibrosis (Figures 1 and 2). However, as shown by Masson trichrome staining and immunohistochemical staining of α-smooth muscle actin (αSMA) in liver tissue, as well as by liver hydroxyproline quantitative measurement results, BDL significantly exacerbated liver fibrosis in the HC diet group as compared with the control (Figures 1*A* and *B*). The messenger RNA (mRNA) expressions of collagen 1α1, collagen 1α2, and αSMA were significantly enhanced with the development of BDL-induced liver fibrosis, which was more evident in the HC diet group than in the control group (Figure 1*C*). TGFβ mRNA levels showed no significant differences between the diet groups (Figure 1*C*). In a similar manner to the BDL model, the murine CCl_4 model of liver fibrosis showed a significant progression of liver fibrosis in the HC diet group vs control (Figures 1*D* and *E*). The mRNA expression of collagen 1α1, collagen 1α2, and αSMA was significantly promoted as a result of the development of CCl_4-induced liver fibrosis, and this was seen more clearly in the HC diet group than in the control group (Figure 1*F*). TGFβ mRNA levels showed no significant between-group differences (Figure 1*F*).

HC Diet Did Not Accelerate BDL- or CCl_4-Induced Hepatocellular Damage

Hepatic TC levels were increased significantly by HC diet consumption for both the BDL and sham groups (Figure 2*A*). However, liver TG levels showed no significant difference between the HC and control groups, and HC diet did not cause hepatic steatosis (Figures 1*A* and 2*A*).

Serum alanine aminotransferase (ALT) levels, a biological marker of hepatocellular damage, were increased significantly in BDL-treated mice; however, this increase was not dependent on dietary cholesterol intake for either the sham or BDL group (Figure 2*B*). In addition, the HC diet did not significantly impact the mitochondrial inner membrane potentials or the numbers of terminal deoxynucleotidyl transferase–mediated deoxyuridine nick-end labeling–positive hepatocytes in the livers of BDL mice (Figure 2*C*).

Hepatic TC levels were increased significantly by consumption of the HC diet vs the control diet for both the CCl_4- and corn oil–treated groups (Figure 2*D*). However, liver TG levels showed no significant difference between the HC and control groups, and the HC diet did not cause hepatic steatosis (Figures 1*D* and 2*D*).

Treatment with CCl_4 significantly increased serum ALT levels relative to treatment with corn oil; however, consumption of the HC diet did not influence serum ALT levels in either the corn oil or CCl_4 group when compared with the control diet (Figure 2*E*). The HC diet did not significantly change the mitochondrial inner membrane potentials or the numbers of terminal deoxynucleotidyl transferase–mediated deoxyuridine nick-end labeling–positive hepatocytes in the livers of CCl_4-treated mice (Figure 2*F*).

In addition, the HC diet did not aggravate acute BDL- or CCl_4-induced hepatocellular damage, even at the time point when liver injury is known to peak (Supplementary Figures 1*A* and *B* and 2*A* and *B*).

These results show that the increase in hepatic cholesterol levels induced by intake of an HC diet did not aggravate BDL- or CCl_4-induced hepatocellular damage.

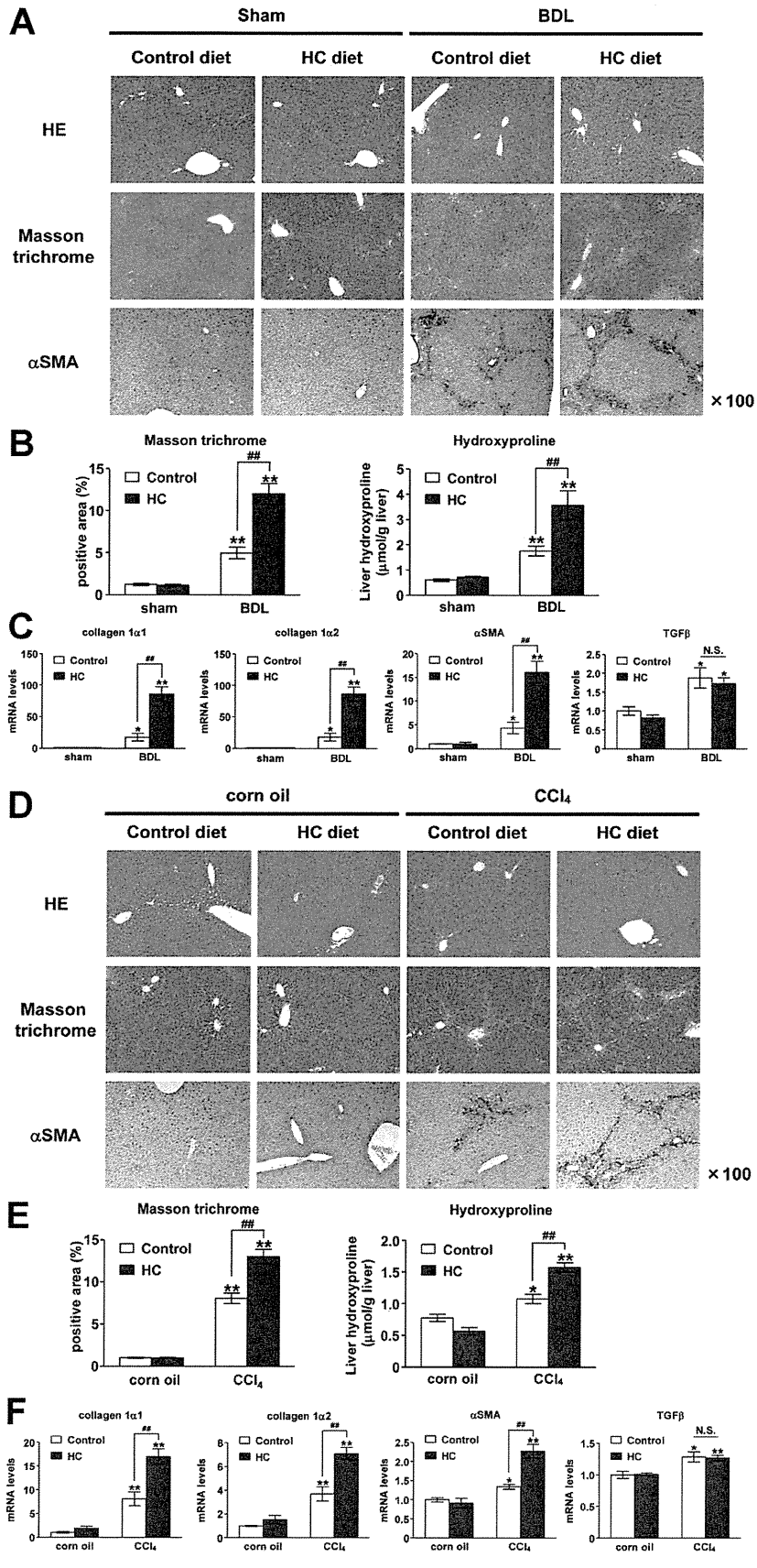

Figure 1. Effects of the HC diet on liver fibrosis induced by BDL or CCl_4 treatment. After being fed a control or HC diet for 4 weeks, C57BL/6 mice were subjected to (*A–C*) 3-week BDL or (*D–F*) CCl_4 treatment twice a week for 4 weeks to induce liver fibrosis (N = 5–7/group). (*A* and *D*) H&E-stained sections, Masson trichrome-stained sections, and immunohistochemical detection of αSMA in representative liver samples. (*B* and *E*) Quantification of Masson trichrome staining (left panel), and liver hydroxyproline concentrations (right panel). (*C* and *F*) Hepatic expression of collagen1α1, collagen1α2, αSMA, and TGFβ mRNA (N = 5/group). $^{*}P < .05$ and $^{**}P < .01$ compared with the (*B* and *C*) control diet–sham-operated group or the (*E* and *F*) control diet–corn oil group. $^{\#\#}P < .01$ compared with the (*B* and *C*) control diet-BDL group or the (*E* and *F*) control diet–CCl_4 group.

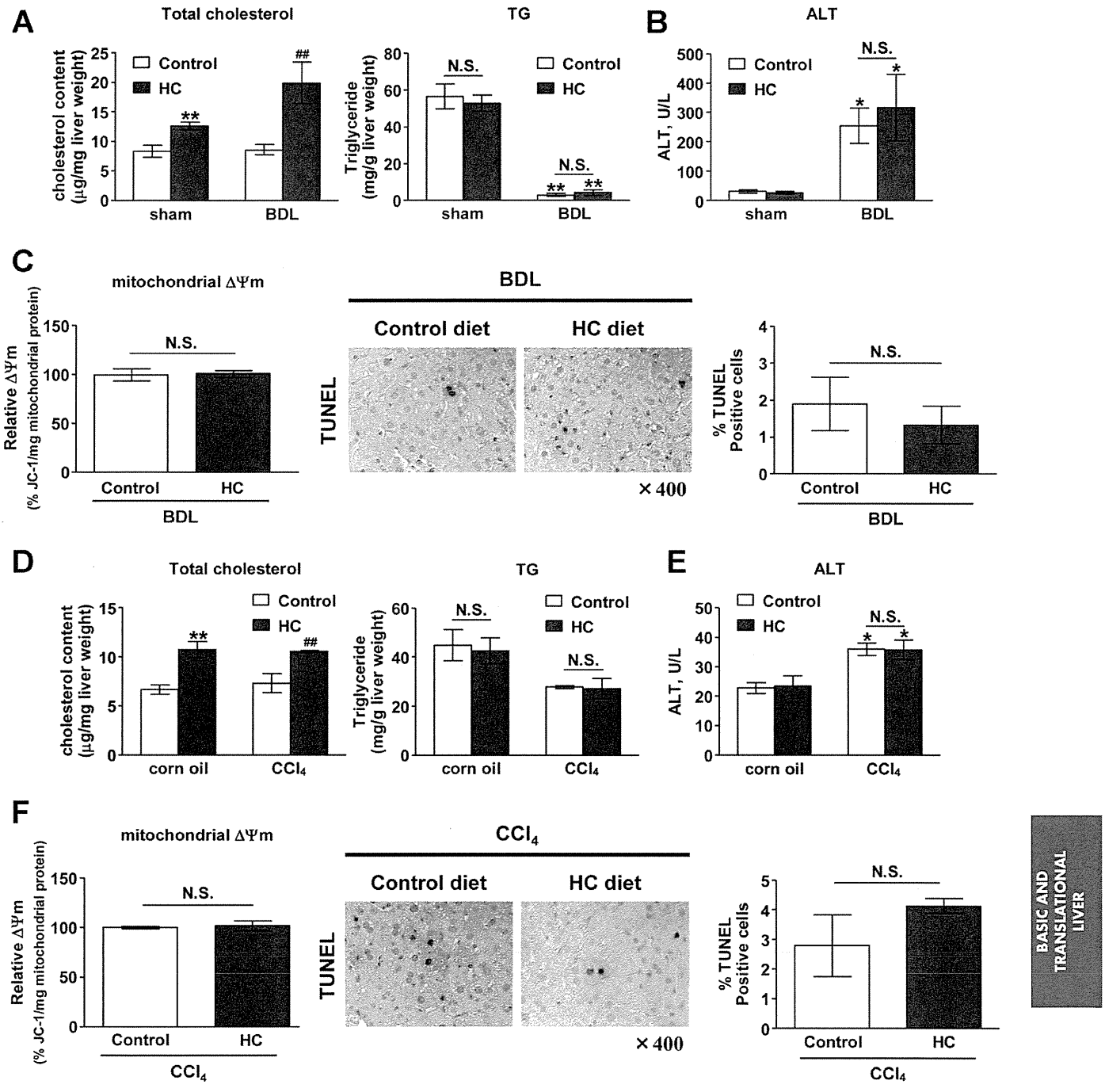

Figure 2. Effects of HC diet on hepatocyte injury induced by BDL or CCl_4 treatment. (*A* and *D*) Hepatic TC and TG contents (N = 5–7/group). (*B* and *E*) Serum ALT activities (N = 5–7/group). (*C* and *F*, *left panels*) Electrochemical proton gradient ($\Delta\Psi$) of the inner mitochondrial membrane (N = 5/group) (*C*, BDL-treated groups; *F*, CCl_4-treated groups). The calculated relative $\Delta\Psi$ was normalized to the values obtained in mice from the (*C*) control diet-BDL group or the (*F*) control diet-CCl_4 group. (*C* and *F*, *right panels*) The percentage of terminal deoxynucleotidyl transferase–mediated deoxyuridine nick-end labeling (TUNEL)-positive hepatocytes and the representative sections (N = 5–7/group). $^{*}P < .05$ and $^{**}P < .01$ compared with the (*A* and *B*) control diet–sham-operated group or the (*D* and *E*) control diet–corn oil group. $^{\#\#}P < .01$ compared with the (*A*) control diet-BDL group or the (*D*) control diet–CCl_4 group.

HC Diet Did Not Impact BDL- or CCl_4-Induced Kupffer Cell Activation or Liver Inflammation

Hepatic macrophage infiltration was evaluated by immunohistochemical staining using the Kupffer cell/macrophage marker F4/80 antibody. The results show BDL-enhanced infiltration of macrophages into the liver in both control- and HC-diet-fed mice. However, consumption of the HC diet did not influence this infiltration (Figure 3*A* and *B*). Kupffer cells are the major source of

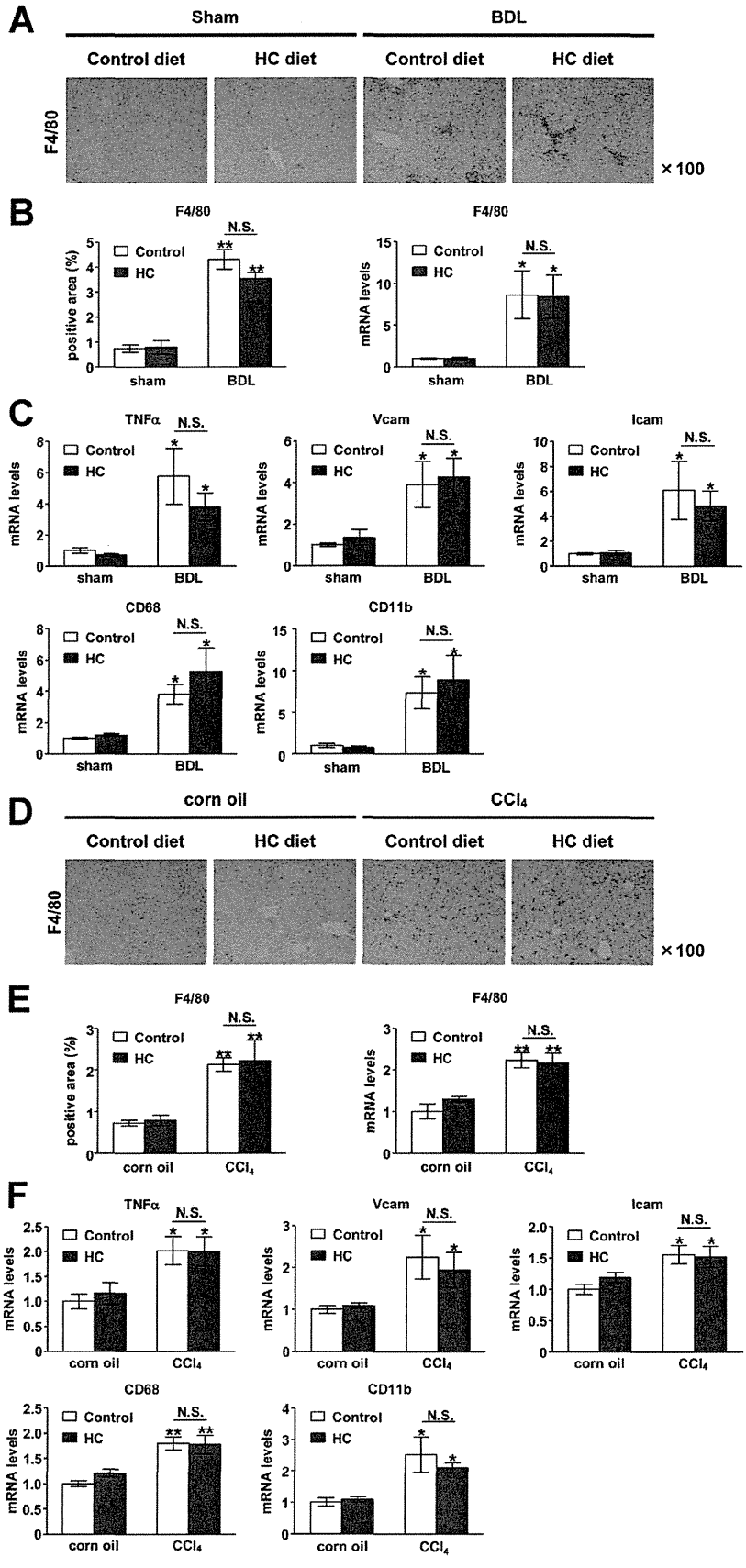

Figure 3. Effects of HC diet on hepatic macrophage infiltration and Kupffer cell activation induced by BDL or CCl_4 treatment. (*A* and *D*) Immunohistochemical detection of F4/80-positive cells in livers. (*B* and *E*) Quantification of F4/80 in immunohistochemical staining and mRNA. (*C* and *F*) Hepatic expression of TNFα, vascular cell adhesion molecule-1 (VCAM-1), intercellular adhesion molecule-1 (ICAM-1), CD68, and CD11b mRNA (N = 5/group). (*A–C*) Sham-operated or BDL groups, and (*D–F*) corn oil or CCl_4-treated groups. *$P < .05$ and **$P < .01$ compared with the (*B* and *C*) control diet–sham-operated group or the (*E* and *F*) control diet–corn oil group.

tumor necrosis factor-α (TNFα) production in the liver. Although BDL significantly promoted TNFα mRNA expression in the liver, the HC diet did not accelerate TNFα genetic expression. In addition, although BDL significantly increased mRNA expression of vascular cell adhesion molecule-1, intercellular adhesion molecule-1, CD68, and CD11b, this increase was not impacted by consumption of the HC diet (Figure 3*C*).

Mice treated with CCl_4 showed enhanced hepatic macrophage infiltration, similar to those treated with BDL. However, consumption of the HC diet did not impact the CCl_4-mediated hepatic macrophage infiltration (Figure 3*D* and *E*). Treatment with CCl_4 significantly increased hepatic levels of TNFα, vascular cell adhesion molecule-1, intercellular adhesion molecule-1, CD68, and CD11b mRNA; however, these levels were not influenced by HC diet consumption (Figure 3*F*). In addition, the HC diet did not influence acute BDL- or CCl_4-induced liver inflammation, even at the time point when liver inflammation peaks (Supplementary Figures 1*C–E* and 2*C–E*).

These results show that the HC diet used in this study did not influence the activation of Kupffer cells or the recruitment of macrophages to the liver. In addition, the HC diet did not impact the BDL- or CCl_4-mediated infiltration of inflammatory cells such as T cells and neutrophils into the liver (Supplementary Figure 3). H&E staining and immunohistochemical staining for CD68 also showed that the HC diet did not induce the formation of hepatic macrophage foam cells or cause liver inflammation (Figure 1*A* and *D* and Supplementary Figure 4).

HC Diet-Induced Aggravation of Liver Fibrosis Was Kupffer Cell–Independent

To determine whether the aggravation of liver fibrosis resulting from HC diet consumption required the presence of Kupffer cells, mice depleted of Kupffer cells with liposomal clodronate were treated with BDL or CCl_4 intoxication. In the BDL model, liposomal clodronate achieved almost complete depletion of Kupffer cells (Figure 4*A*), along with suppression of proinflammatory cytokines such as TNFα and interleukin-1β (Supplementary Figure 5*A*). Treatment with liposomal clodronate did not impact the BDL-induced hepatocellular injury (Figure 4*A*, bottom row). In mice treated with liposomal clodronate, intake of the HC diet significantly promoted the BDL-induced aggravation of liver fibrosis (Figure 4*B*). In agreement with these results, mice treated with liposomal clodronate showed a significant increase in BDL-induced expression of collagen 1α1, collagen 1α2, and αSMA in the liver when fed an HC diet (Figure 4*C*).

Similarly, treatment with liposomal clodronate almost completely depleted Kupffer cells in the CCl_4 model (Figure 4*D*), and also suppressed proinflammatory cytokines such as TNFα and interleukin-1β (Supplementary Figure 5*B*). Administration of liposomal clodronate did not impact the CCl_4-induced hepatocellular injury (Figure 4*D*, bottom row). In mice infused with liposomal clodronate, the HC diet significantly boosted the CCl_4-induced progression of liver fibrosis (Figure 4*E*). In accord with these findings, mice dosed with liposomal clodronate showed a significant increase in CCl_4-induced mRNA expression of collagen 1α1, collagen 1α2, and αSMA in the liver when administered the HC diet (Figure 4*F*).

These results suggested that the HC diet promoted BDL- and CCl_4-induced liver fibrosis in a Kupffer cell–independent manner.

Accumulation of Free Cholesterol Sensitized HSCs to TGFβ-Induced Activation

To examine the effects of the HC diet on HSCs, these cells were isolated from mice given the control or HC diets. With HSCs from the control diet group, the mean (±SD) TC content was 28.94 ± 11.55 μg/mg cell protein. In HSCs from the HC diet group, the mean (±SD) TC content was increased significantly to 59.90 ± 22.93 μg/mg cell protein. In addition, free cholesterol (FC) and cholesterol ester (CE) levels in HSCs were determined. Consequently, FC levels were significantly higher in the HC diet group HSCs than in those from the control diet group; however, no significant difference was noted in the CE level between groups (Figure 5*A*).

Second, to investigate the effects of HC diet on HSC activation, HSCs isolated from mice from both groups were stimulated with profibrogenic cytokine TGFβ. Samples of HSCs before treatment with TGFβ, collected from mice, showed that the HC diet did not affect mRNA levels of collagen 1α1, collagen 1α2, or αSMA. Treatment with TGFβ significantly enhanced the levels of collagen 1α1, collagen 1α2, and αSMA mRNA transcripts in HSCs. The enhancing effect was noted more prominently in the HC diet group than in controls (Figure 5*B*, top row). The HSC expression levels of TGFβ receptor-1 and TGFβ receptor-2 (regulating sensitivity to TGFβ) and the TGFβ pseudoreceptor Bambi were compared quantitatively between the 2 diet groups. Expression of Bambi was significantly lower in the HC diet group than the control group (Figure 5*B*, bottom row), however, no significant difference was observed in the expression levels of the TGFβ receptors between groups. In accord with these findings, hepatic expression of Bambi mRNA also was significantly lower in the HC diet group than in the control group (Supplementary Figure 6).

Third, the effect of FC on the HSC sensitivity to TGFβ was evaluated. Niemann-Pick C1 (NPC1) is a late endosomal protein that regulates intracellular cholesterol transport. Homozygous NPC1-deficient cells have been shown to accumulate intracellular FC.[9,10] Therefore, HSCs isolated from NPC1 knock-out (KO) mice were used for analysis. Before treatment with TGFβ, no significant differences were found between WT and NPC1 KO HSCs in the expression levels of collagen 1α1, collagen 1α2, or αSMA mRNA transcripts. Treatment with TGFβ significantly increased the levels of collagen 1α1, collagen 1α2, and αSMA mRNA transcripts. The positive effect was seen more markedly in NPC1 KO HSCs than in WT HSCs (Figure 5*C*, *left three panels*). Bambi mRNA levels were

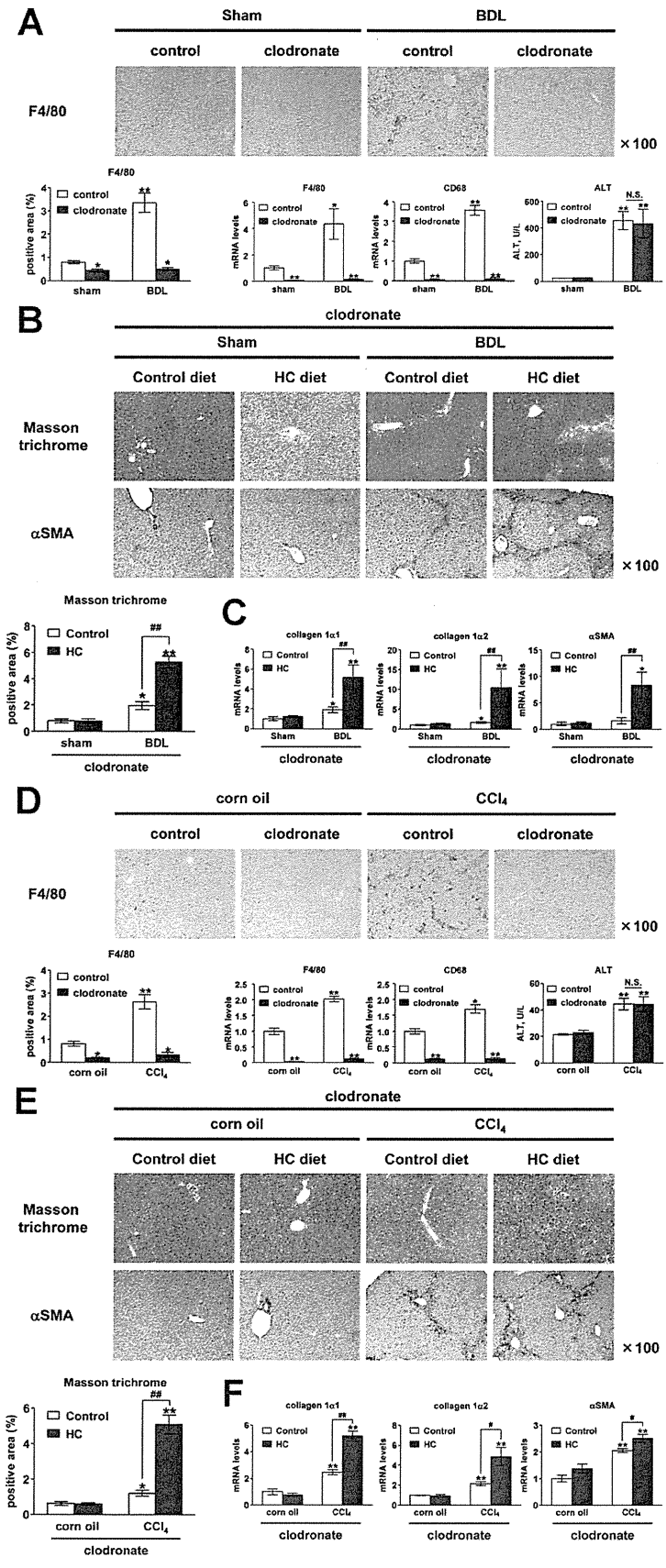

Figure 4. Depletion of Kupffer cells does not abrogate the effects of the HC diet on hepatic fibrosis induced by BDL or CCl_4 treatment. WT C57BL/6 mice were injected with liposomal clodronate or vehicle. Thereafter, animals were subjected to (*A–C*) BDL or (*D–F*) CCl_4 intoxication to induce liver fibrosis. (*A* and *D*, *upper panels*) Immunohistochemical staining for F4/80. (*A* and *D*, *lower panels*) Quantification of immunohistochemical staining for F4/80 (*left*). Hepatic expression of F4/80 and CD68 mRNA (N = 4−7/group) (*middle*), and serum ALT levels (*right*). $^{*}P < .05$ and $^{**}P < .01$ compared with the (*A*) vehicle-treated–sham-operated group or the (*D*) vehicle-treated–corn oil group. (*B* and *E*, *upper panels*) Masson trichrome staining. (*B* and *E*, *middle panels*) Immunohistochemical detection of αSMA. (*B* and *E*, *lower panels*) Quantification of Masson trichrome staining. (*C* and *F*) Hepatic expression of collagen 1α1, collagen 1α2, and αSMA mRNA (N = 4−7/group). $^{*}P < .05$ and $^{**}P < .01$ compared with the (*B* and *C*) control diet–sham-operated group or the (*E* and *F*) control diet–corn oil group. $^{\#}P < .05$ and $^{\#\#}P < .01$ compared with the (*B* and *C*) control diet–BDL group or the (*E* and *F*) control diet–CCl_4 group.

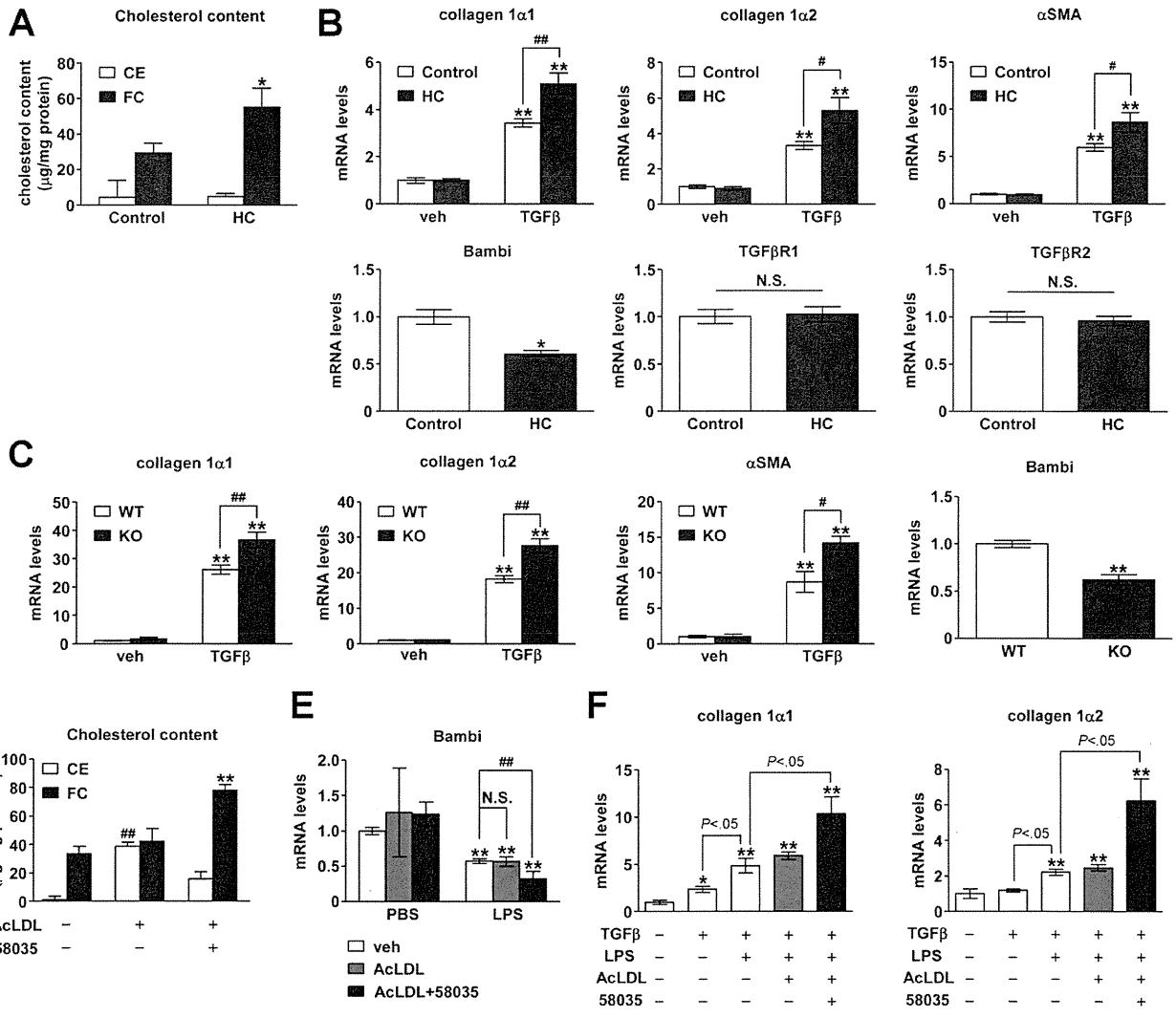

Figure 5. FC, but not CE, promotes TGFβ-induced HSC activation. (*A*) Quantification of cellular FC and CE in HSCs immediately after isolation from control diet–fed or HC diet–fed mice (N = 5–7/group). $^{*}P < .05$ vs control-diet group. (*B*) Expression of (*upper panels*) collagen 1α1, collagen 1α2, αSMA, and (*lower panels*) Bambi, TGFβR1, and TGFβ R2 mRNA in primary HSC cultures. (*Upper panels*) Primary HSCs isolated from control diet–fed or HC diet–fed mice were treated or not treated with TGFβ (1 ng/mL) for 6 hours. (*Lower panels*) HSCs separated from control diet–fed or HC diet–fed mice were analyzed with real-time polymerase chain reaction (N = 5–7/group). $^{*}P < .05$ and $^{**}P < .01$ vs the control diet–control culture. $^{\#}P < 0.05$ and $^{\#\#}P < 0.01$ vs the control diet–TGFβ-treated culture. (*C*) Expression of (*left three panels*) collagen 1α1, collagen 1α2, αSMA, and (*far right panel*) Bambi mRNA in primary HSC cultures. (*Left three panels*) Primary HSCs isolated from WT mice or NPC1-deficient mice were treated with TGFβ (1 ng/mL) or not for 6 hours. (*Far right panel*) HSCs separated from WT mice or NPC1-deficient mice were analyzed by real-time polymerase chain reaction (N = 5–7/group). $^{**}P < 0.01$ vs the WT mice–control culture. $^{\#}P < .05$ and $^{\#\#}P < .01$ vs the WT mice–TGFβ-treated culture. (*D*) Quantification of cellular FC and CE in primary cultured HSCs. HSCs were incubated with vehicle, AcLDL (50 μg/mL), or AcLDL plus compound 58035 (10 μg/mL) for 16 hours (N = 5–7/group). $^{**}P < .01$ vs cellular FC content in the vehicle-treated culture. $^{\#\#}P < .01$ vs cellular CE content in the vehicle-treated culture. (*E*) Expression of Bambi mRNA in primary HSC cultures. HSCs were incubated with vehicle, AcLDL, or AcLDL plus compound 58035 for 16 hours, and then treated with LPS (100 ng/mL) or not for 6 hours (N = 5–7/group). $^{**}P < .01$ vs the corresponding culture without LPS treatment in each group. $^{\#\#}P < .01$ vs the LPS-treated control culture. (*F*) Expression of collagen 1α1 and collagen 1α2 mRNA in primary HSC cultures. HSCs were incubated with vehicle, AcLDL, or AcLDL plus compound 58035 for 16 hours, and then treated with LPS (100 ng/mL) or not for 6 hours, before the addition of TGFβ for an additional 6 hours (N = 5–7/group). $^{*}P < .05$ and $^{**}P < .01$ vs the vehicle-treated control culture.

significantly lower in NPC1 KO HSCs relative to WT HSCs (Figure 5*C, far right panel*). It has been reported that cholesterol accumulates predominantly in late endosomes/lysosomes of cells in NPC1 KO mice.[9] Our study also found that FC levels in late endosomes/lysosomes were significantly higher in NPC1 KO HSCs than in WT HSCs (Supplementary Figure 7*A*). Similarly, FC levels in late endosomes/lysosomes were significantly higher in the HSCs from the HC diet group than in those from the control diet group (Supplementary Figure 7*B*).

It has been reported that FC accumulates in cells treated with the combination of acetyl low-density lipoprotein (AcLDL) and acyl-CoA:cholesterol acyltransferase inhibitor 58035 (compound 58035), whereas CE accumulates in cells

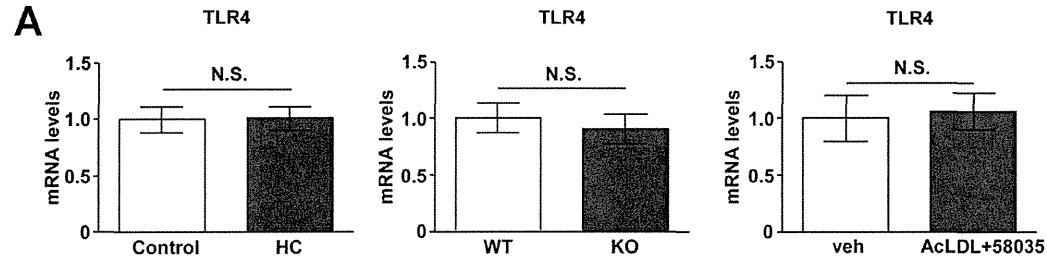
A
TLR4
TLR4
TLR4
mRNA levels
N.S.
Control
HC
WT
KO
veh
AcLDL+58035

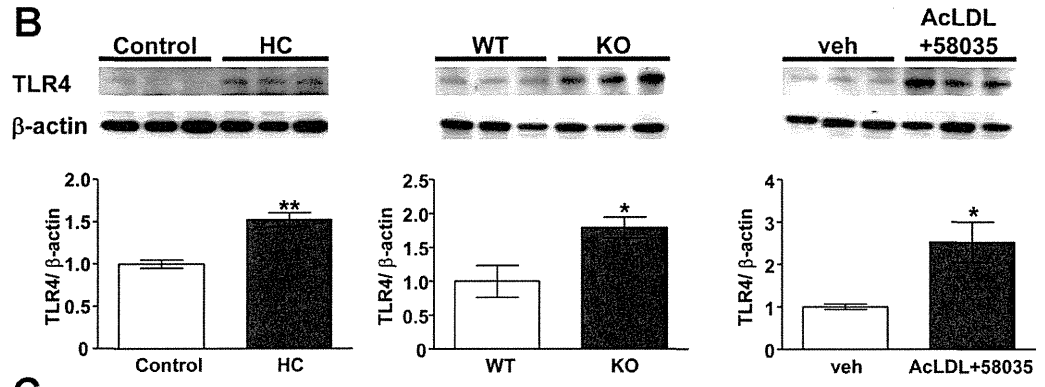
B
Control
HC
WT
KO
veh
AcLDL +58035
TLR4
β-actin
TLR4/ β-actin

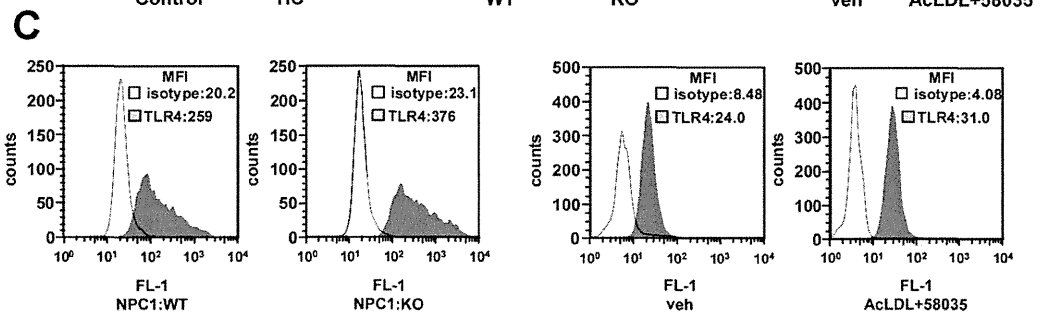
C
MFI
isotype:20.2
TLR4:259
isotype:23.1
TLR4:376
isotype:8.48
TLR4:24.0
isotype:4.08
TLR4:31.0
counts
FL-1
NPC1:WT
NPC1:KO
veh
AcLDL+58035

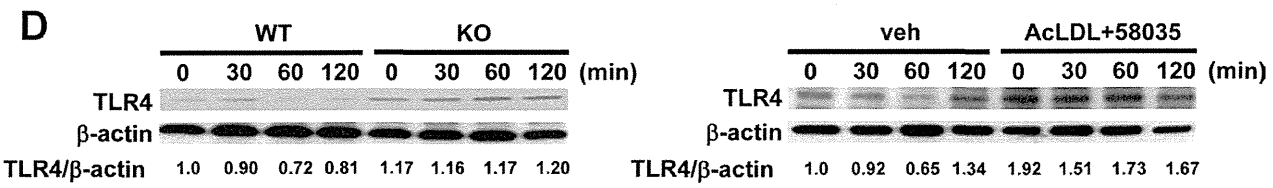
D
WT
KO
veh
AcLDL+58035
0 30 60 120 0 30 60 120 (min)
TLR4
β-actin
TLR4/β-actin
1.0 0.90 0.72 0.81 1.17 1.16 1.17 1.20
1.0 0.92 0.65 1.34 1.92 1.51 1.73 1.67

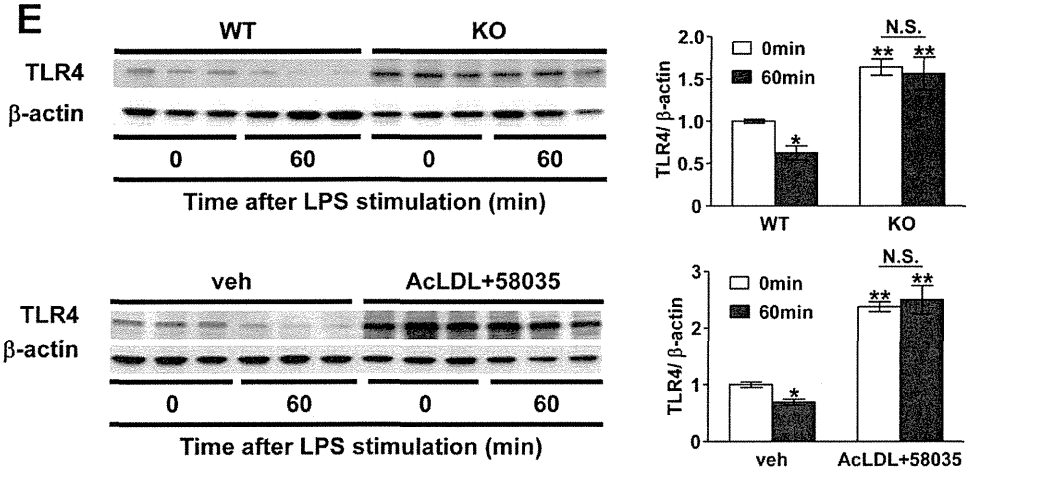
E
WT
KO
TLR4
β-actin
0 60 0 60
Time after LPS stimulation (min)
0min
60min
N.S.
TLR4/ β-actin
veh
AcLDL+58035

treated with AcLDL alone.[11] In our study, treatment of HSCs with AcLDL plus compound 58035 significantly increased FC accumulation, and treatment with AcLDL alone significantly promoted CE accumulation (Figure 5*D*). However, the Bambi expression levels were not decreased when HSCs were treated with either AcLDL alone or the combination of AcLDL and compound 58035 (Figure 5*E*). The expression of the Bambi gene in HSCs has been reported to depend on TLR4 signaling and decreases with the addition of lipopolysaccharide (LPS).[12] In our study as well, Bambi mRNA expression levels were decreased significantly when HSCs were treated with LPS (Figure 5*E*). The decrease in Bambi mRNA levels was enhanced significantly when cells were treated with AcLDL plus compound 58035, whereas cells treated with AcLDL alone did not show a significant reduction compared with controls (Figure 5*E*). The accumulation of FC in HSCs also intensified LPS-mediated TLR4 signal transduction to induce proinflammatory cytokines such as monocyte chemoattractant protein-1 and macrophage inflammatory protein-2 (Supplementary Figures 8*A* and *B*), which are known to be up-regulated by the LPS-mediated TLR4 signal pathway in HSCs.[12,13] HSCs pretreated with LPS showed a significant enhancement of collagen 1α1 and 1α2 mRNA expression when stimulated with TGFβ (Figure 5*F*). These cells showed a further increase in the mRNA expression of these genes when loaded with AcLDL plus compound 58035, whereas no significant increase was observed when cells were incubated with AcLDL alone (Figure 5*F*). These results clearly indicate that FC accumulation in HSCs sensitized them to TGFβ-induced signals by down-regulating Bambi gene expression.

Unlike HSCs, there were no significant differences in Kupffer cell FC levels between the HC diet group and the control diet group; however, CE levels were significantly higher in Kupffer cells from the HC diet group than in those from the control diet group (Supplementary Figure 9*A*). An accumulation of CE did not accelerate TNFα mRNA expression in Kupffer cells (Supplementary Figure 9*B*), nor did it enhance LPS-induced TNFα mRNA expression in these cells (Supplementary Figure 9*B*). These results show that the HC diet did not cause Kupffer cells to trigger hepatic fibrosis, although it did increase Kupffer cell CE levels.

Accumulation of FC in HSCs Up-Regulated TLR4 Expression

Consumption of the HC diet did not affect TLR4 mRNA expression levels in HSCs. However, the HC diet increased the amount of TLR4 protein expressed in HSCs (Figure 6*A* and *B*). In addition, increased levels of TLR4 gene expression in terms of the amount of protein (but not mRNA) also were observed in NPC1 KO HSCs and HSCs stimulated with AcLDL plus compound 58035 (Figure 6*A* and *B*). Moreover, NPC1 KO HSCs showed higher TLR4 protein membrane expression relative to WT HSCs (Figure 6*C*). Similar results were obtained for HSCs treated with AcLDL plus compound 58035 (Figure 6*C*).

Under normal conditions, membrane proteins are internalized into the cytoplasm by endocytosis, where they are degraded by endosomal–lysosomal or proteasomal pathways. Ligand formation enhances the endocytotic activity, and, consequently, degradation of membrane proteins is accelerated.[14] To investigate the role of FC in TLR4 expression, we examined the dynamic change in the quantity of TLR4 protein in cells treated with LPS. We found that TLR4 protein expression was decreased 60 minutes after LPS treatments in WT HSCs, whereas that in NPC1 KO HSCs remained at a high level after LPS treatments (Figure 6*D*, *left row*, and *E*, *top row*). Similar results were obtained for HSCs treated with AcLDL plus compound 58035 (Figure 6*D*, *right row*, and *E*, *bottom row*). These results clearly show that HSC accumulation of FC significantly increased TLR4 protein content. We conjectured that intercellular FC accumulation probably suppressed the ligand-mediated enhanced degradation of TLR4.

HC Diet-Induced Aggravation of Liver Fibrosis Was Dependent on TLR4 Signal Transduction in HSCs

In the last part of the experiment, we used LPS-unresponsive C3H/HeJ mice (TLR4 mutant) to assess whether HC diet-induced aggravation of liver fibrosis was dependent on TLR4 signal transduction. Unlike the results obtained with WT mice, HC diet consumption did not enhance the progression of BDL-induced liver fibrosis in C3H/HeJ mice (Figure 7*A* and *B*). Similarly, the HC diet did not hasten the progression of CCl_4-induced liver fibrosis (Figure 7*C* and *D*).

Next, we examined whether HSC activation by accumulated FC required TLR4 signaling in HSCs. Samples of HSCs were collected from C3H/HeJ mice given the control or HC diet for 4 weeks, and used for study. Treatment with TGFβ significantly enhanced the levels of collagen 1α1, collagen 1α2, and αSMA mRNA transcripts in HSCs. However, unlike the results obtained with WT mouse HSCs, no significant difference was found between the HC and control diet

BASIC AND TRANSLATIONAL LIVER

Figure 6. FC enhances protein expression of TLR4 in HSCs. TLR4 (*A*) mRNA and (*B*) protein expression (HSCs isolated from control diet-fed or HC-fed mice [*left*], WT or NPC1-deficient HSCs [*middle*], vehicle-treated or FC-loaded HSCs [*right*]). (*B*, *lower panels*) Quantification of TLR4 protein expression. $^{**}P < .01$ vs control-diet group (*left*); $^{*}P < .05$ vs WT HSCs (*middle*); and $^{*}P < .05$ vs vehicle-treated HSCs (*right*). (*C*) Fluorescence-activated cell sorter assay of TLR4 expression on plasma membranes of WT or NPC1-deficient HSCs (*left*) and vehicle-treated or FC-loaded HSCs (*right*). The mean fluorescence intensity (MFI) is also shown at the upper right corner of each panel. (*D*) Dynamic changes and (*E*) quantification of TLR4 protein expression in WT or NPC1-deficient HSCs (*D, left panels; E, upper panels*), and vehicle-treated or FC-loaded HSCs (*D, right panels; E, lower panels*) shown at the time after LPS (100 ng/mL) treatment. The relative levels of TLR4 to β-actin are indicated below the corresponding bands. $^{*}P < .05$ and $^{**}P < .01$ vs the WT HSCs or vehicle-treated HSCs before LPS treatment. HSCs cultured 6 days after isolation from mice or rats were used (*C–E*).

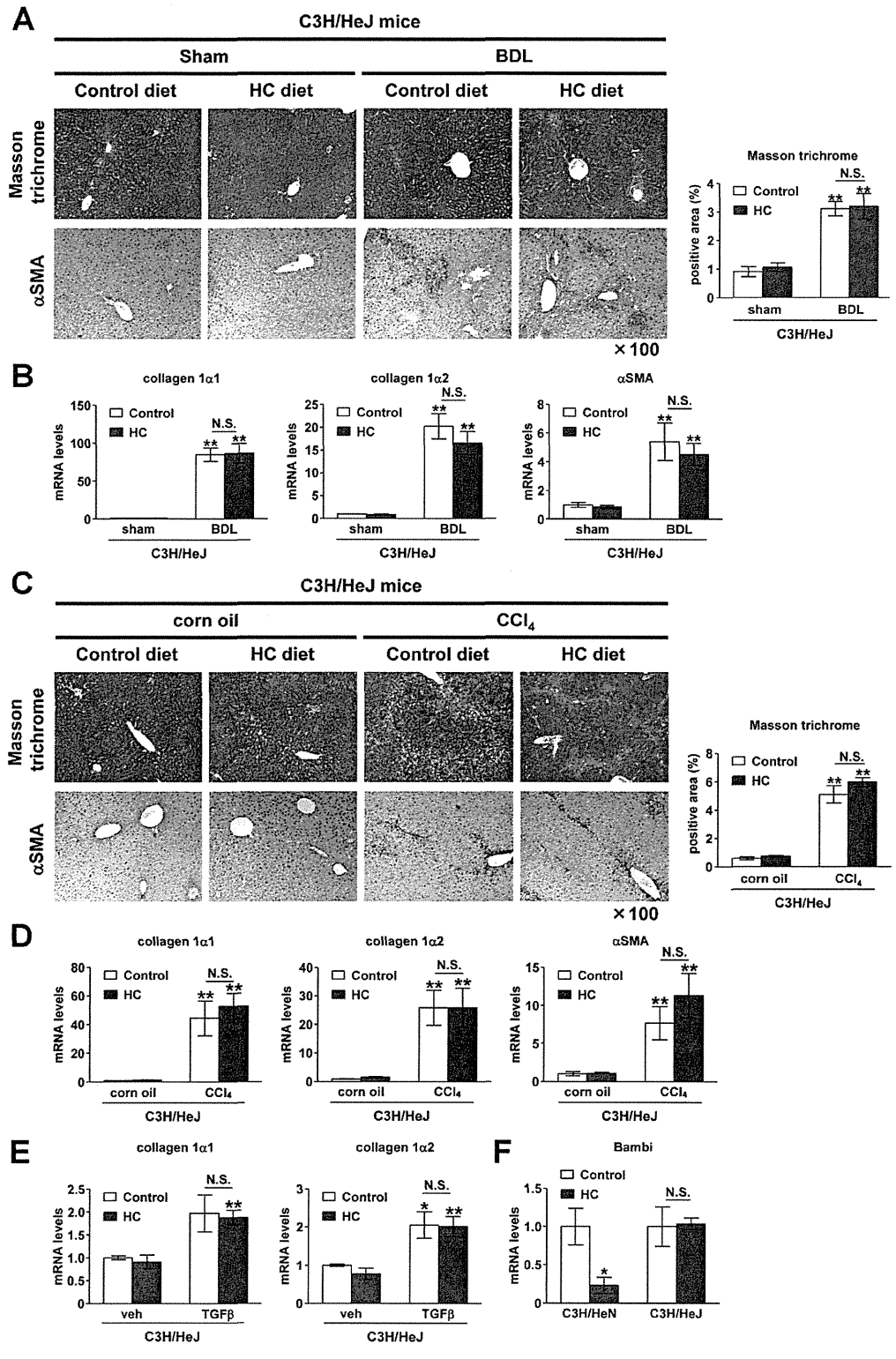

Figure 7. HC diet–induced aggravation of liver fibrosis was dependent on TLR4 signal transduction in HSCs. TLR4 mutant (C3H/HeJ) mice were fed a control or HC diet for 4 weeks. Then, while remaining on the same diet, animals were subjected to (*A* and *B*) BDL or (*C* and *D*) CCl_4 intoxication for induction of liver fibrosis (N = 4–7/group). (*A* and *C*) Masson trichrome staining (*left upper panels*) and immunohistochemical staining for α-SMA (*left lower panels*). Quantification of Masson trichrome staining (*right panels*). (*B* and *D*) Hepatic expression of collagen 1α1, collagen 1α2, and αSMA mRNA (N = 4–7/group). $^{**}P < .01$ compared with the (*B*) control diet–sham-operated group or the (*D*) control diet–corn oil group. (*E*) Expression of collagen 1α1 and collagen 1α2 mRNA in primary HSCs. HSCs isolated from control diet–fed or HC diet–fed C3H/HeJ mice were treated or not treated with TGFβ (1 ng/mL) for 6 hours (N = 5–7/group). $^{*}P < .05$ and $^{**}P < .01$ vs the control diet–control culture. (*F*) Expression of Bambi mRNA in primary HSCs isolated from C3H/HeN mice or C3H/HeJ mice, fed a control or an HC diet (N = 5–7/group). $^{*}P < .05$ vs the control diet–C3H/HeN mice group.

groups (Figure 7*E*). Moreover, although HC diet consumption significantly attenuated Bambi gene expression in HSCs isolated from C3H/HeN mice (WT control for C3H/HeJ mice), the HSC Bambi mRNA level was not affected in C3H/HeJ mice (Figure 7*F*).

These findings clearly show that HC diet-induced aggravation of liver fibrosis was dependent on TLR4 signal transduction. Our study suggested that HC diet consumption attenuated HSC Bambi expression via TLR4 signaling, which led to the aggravation of BDL- or CCl_4-induced liver fibrosis.

Discussion

Our present results clearly show that an HC diet aggravated BDL- and CCl_4-induced liver fibrosis, although an HC diet alone was not sufficient for inducing liver fibrosis. TGFβ, the most potent factor predisposing to human fibrogenesis, has been shown to play a central role in the pathophysiology of liver fibrosis.[1] Moreover, these results showed that major causes for exacerbation of liver fibrosis involved HSC accumulation of cholesterol in the form of FC, which sensitized HSCs to TGFβ-induced activation.

Recent research has shown that intracellular FC accumulation increased TLR4 protein levels in the membrane fraction to facilitate TLR4 signaling activation.[15] Our results showed that HSC accumulation of FC increased cytomembrane-bound TLR4 protein levels; however, the amounts of TLR4 mRNA transcripts were similar. Under normal conditions, cytomembrane TLR4 protein molecules are transferred into the cytoplasm by endocytosis, and degraded by endosomal–lysosomal or proteasomal pathways. Degradation of cytomembrane TLR4 proteins is accelerated when internalization of these molecules is promoted by ligand formation. Inhibition of the degradation pathways intensifies ligand-mediated TLR4 signal transduction.[14] In our study, the level of the TLR4 protein in HSCs was lowered significantly in cells incubated with LPS, the major ligand for TLR4. Moreover, the LPS-induced decrease in the HSC level of the TLR4 protein was inhibited prominently by FC accumulated in HSCs. These results suggest that FC accumulated in HSCs inhibited the TLR4 degradation pathway, thereby increasing TLR4 protein levels.

In the present study, FC levels in late endosomes/lysosomes were significantly higher in HSCs from the HC diet group or NPC1 KO mice than in those from the control diet group or WT mice. Recent studies have reported that FC modulated the endosomal–lysosomal pathway of endocytosis through regulation of endosome motility.[16] NPC1 KO mice, which accumulate intracellular FC predominantly in late endosomes/lysosomes, were found to retain amyloid precursor proteins as a result of endosomal dysfunction.[9] NPC1 KO mice also were found to show autophagic–lysosomal dysfunction in the brain.[10] These findings suggest that FC accumulation in HSCs is involved in endosomal–lysosomal dysfunction, leading to TLR4 protein accumulation.

The expression of the TGFβ pseudoreceptor Bambi in HSCs was solely dependent on TLR4 signaling.[12] The activation of TLR4 signaling in HSCs, which down-regulates the expression of the downstream Bambi gene, was reported to sensitize HSCs to TGFβ-induced activation, contributing to advancement of liver fibrosis.[12] In our study, HSCs also showed a significantly decreased expression of the Bambi gene when incubated with the TLR4 ligand LPS. The HSC accumulation of FC (not CE) significantly promoted LPS-mediated Bambi down-regulation and markedly accelerated (LPS-mediated) enhancement of HSC sensitivity against TGFβ signaling. We contend that these changes activated HSCs further, thereby promoting liver fibrosis.

In our experiment, TLR4-mutant C3H/HeJ mice given the HC diet did not show aggravation of liver fibrosis. Accumulation of FC in HSCs collected from TLR4-mutant mice did not give rise to Bambi down-regulation, and no change was observed in the HSC sensitivity against TGFβ signaling. Based on these results, we concluded that the activation of the TLR4 signal pathway mediated by FC accumulated in HSCs played a critical role in HC diet-induced exacerbation of liver fibrosis.

In the murine liver fibrosis models reported here, consumption of an HC diet neither affected hepatocyte injury nor influenced the pathophysiology of liver inflammation, including Kupffer cell activation.

Marí et al[17] found that FC accumulated in hepatocytes exacerbated LPS-mediated acute liver injury in a manner that induced susceptibility of hepatocytes to TNFα-mediated apoptosis. However, several other researchers claimed that TNFα-mediated hepatocyte apoptosis was not involved in the progression of liver fibrosis,[18,19] and their findings seem to shed light on the reason why cholesterol accumulation in hepatocytes resulting from consumption of an HC diet did not significantly exacerbate hepatocyte damage, as shown in our study. Wouters et al[20] reported that administration of a high-fat HC diet in low-density lipoprotein receptor KO and apolipoprotein E KO mice caused liver inflammation and the transformation of Kupffer cells into foam cells. However, HC diet consumption did not trigger macrophage foam cell formation in the models used in our study. We also clearly showed that an HC diet aggravated BDL- and CCl_4-induced liver fibrosis in mice depleted of Kupffer cells by administration of clodronate. Altogether, these results suggest that HSCs, rather than hepatocytes or Kupffer cells, should be focused on as the primary site of alterations in liver fibrosis resulting from HC diet consumption.

In summary, our study has provided new insights into the mechanisms linking HC diet uptake and liver fibrosis. The HC diet-induced accumulation of FC in HSCs promoted TLR4 signal transduction by increasing membrane TLR4 levels, and thereby suppressed the HSC expression of the Bambi gene. Consequently, HSC TGFβ signaling was boosted, resulting in HSC activation and progression of liver fibrosis.

Our present work indicates that in the process of liver fibrosis progression, cholesterol functions as a signal-enhancing factor FC that accumulates in HSCs, rather than as an extracellular activation-inducible factor for HSCs. The findings of this study warrant further investigations that focus on FC in HSCs as the target of new therapeutic strategies for the treatment of liver fibrosis.

Supplementary Material

Note: To access the supplementary material accompanying this article, visit the online version of

Gastroenterology at www.gastrojournal.org, and at doi: 10.1053/j.gastro.

References

1. Friedman SL. Mechanisms of hepatic fibrogenesis. Gastroenterology 2008;134:1655–1669.
2. Ioannou GN, Morrow OB, Connole ML, et al. Association between dietary nutrient composition and the incidence of cirrhosis or liver cancer in the United States population. Hepatology 2009;50: 175–184.
3. Ekstedt M, Franzén LE, Mathiesen UL, et al. Statins in non-alcoholic fatty liver disease and chronically elevated liver enzymes: a histopathological follow-up study. J Hepatol 2007;47: 135–141.
4. Yoneda M, Fujita K, Nozaki Y, et al. Efficacy of ezetimibe for the treatment of non-alcoholic steatohepatitis: an open-label, pilot study. Hepatol Res 2010;40:613–621.
5. Sumiyoshi M, Sakanaka M, Kimura Y. Chronic intake of a high-cholesterol diet resulted in hepatic steatosis, focal nodular hyperplasia and fibrosis in non-obese mice. Br J Nutr 2010;103:378–385.
6. Kainuma M, Fujimoto M, Sekiya N, et al. Cholesterol-fed rabbit as a unique model of nonalcoholic, nonobese, non-insulin-resistant fatty liver disease with characteristic fibrosis. J Gastroenterol 2006;41:971–980.
7. Vergnes L, Phan J, Strauss M, et al. Cholesterol and cholate components of an atherogenic diet induce distinct stages of hepatic inflammatory gene expression. J Biol Chem 2003;278: 42774–42784.
8. Malhi H, Bronk SF, Werneburg NW, et al. Free fatty acids induce JNK-dependent hepatocyte lipoapoptosis. J Biol Chem 2006;281: 12093–12101.
9. Jin LW, Shie FS, Maezawa I, et al. Intracellular accumulation of amyloidogenic fragments of amyloid-beta precursor protein in neurons with Niemann-Pick type C defects is associated with endosomal abnormalities. Am J Pathol 2004;164:975–985.
10. Liao G, Yao Y, Liu J, et al. Cholesterol accumulation is associated with lysosomal dysfunction and autophagic stress in Npc1 −/− mouse brain. Am J Pathol 2007;171:962–975.
11. Li Y, Schwabe RF, DeVries-Seimon T, et al. Free cholesterol-loaded macrophages are an abundant source of tumor necrosis factor-alpha and interleukin-6: model of NF-kappaB- and map kinase-dependent inflammation in advanced atherosclerosis. J Biol Chem 2005;280:21763–21772.
12. Seki E, De Minicis S, Osterreicher CH, et al. TLR4 enhances TGF-beta signaling and hepatic fibrosis. Nat Med 2007;13:1324–1332.
13. Paik YH, Schwabe RF, Bataller R, et al. Toll-like receptor 4 mediates inflammatory signaling by bacterial lipopolysaccharide in human hepatic stellate cells. Hepatology 2003;37:1043–1055.
14. Wang Y, Chen T, Han C, et al. Lysosome-associated small Rab GTPase Rab7b negatively regulates TLR4 signaling in macrophages by promoting lysosomal degradation of TLR4. Blood 2007;110:962–971.
15. Suzuki M, Sugimoto Y, Ohsaki Y, et al. Endosomal accumulation of Toll-like receptor 4 causes constitutive secretion of cytokines and activation of signal transducers and activators of transcription in Niemann-Pick disease type C (NPC) fibroblasts: a potential basis for glial cell activation in the NPC brain. J Neurosci 2007; 27:1879–1891.
16. Chen H, Yang J, Low PS, et al. Cholesterol level regulates endosome motility via Rab proteins. Biophys J 2008;94:1508–1520.
17. Marí M, Caballero F, Colell A, et al. Mitochondrial free cholesterol loading sensitizes to TNF- and Fas-mediated steatohepatitis. Cell Metab 2006;4:185–198.
18. Bohan A, Chen WS, Denson LA, et al. Tumor necrosis factor alpha-dependent up-regulation of Lrh-1 and Mrp3(Abcc3) reduces liver injury in obstructive cholestasis. J Biol Chem 2003;278: 36688–36698.
19. Simeonova PP, Gallucci RM, Hulderman T, et al. The role of tumor necrosis factor-alpha in liver toxicity, inflammation, and fibrosis induced by carbon tetrachloride. Toxicol Appl Pharmacol 2001; 177:112–120.
20. Wouters K, van Gorp PJ, Bieghs V, et al. Dietary cholesterol, rather than liver steatosis, leads to hepatic inflammation in hyperlipidemic mouse models of nonalcoholic steatohepatitis. Hepatology 2008;48:474–486.

Received November 13, 2010. Accepted September 24, 2011.

Reprint requests

Address requests for reprints to: Kengo Tomita, MD, PhD, Division of Gastroenterology and Hepatology, Department of Internal Medicine, National Defense Medical College, 3-2 Namiki, Tokorozawa-shi, Saitama 359-8513, Japan. e-mail: kengo@ndmc.ac.jp; fax: (81) 4-2996-5201.

Acknowledgments

The authors thank Mina Kitazume and Miho Takabe (Keio University) for helpful advice and technical assistance; and Drs Shuhji Seki, Manabu Kinoshita, and Hiroyuki Nakashima (Department of Immunology and Microbiology, National Defense Medical College) for helpful discussion and critical comments.

T. Teratani and K. Tomita contributed equally to this work and share first authorship.

Conflicts of interest

The authors disclose no conflicts.

Funding

This study was supported in part by a Grant-in-Aid for Scientific Research from the Ministry of Education, Culture, Sports, Science, and Technology of Japan (to K. Tomita).

Supplementary Materials and Methods

Reagents

Reagents were obtained as follows: AcLDL was from Biomedical Technologies (Stoughton, MA). Compound 58035 and LPS were from Sigma (St. Louis, MO). TGFβ was from R&D Systems (Minneapolis, MN). CCl_4 was from Wako Pure Chemical Industries (Osaka, Japan).

Animal Model

Male WT C57BL/6, C3H/HeN, and C3H/HeJ mice and Sprague-Dawley rats were purchased from Sankyo Laboratories (Tokyo, Japan). NPC1$^{-/-}$ mice were purchased from Jackson Laboratories (Bar Harbor, ME). Mice were bred and housed in a temperature- and light-controlled facility with unlimited access to food and water. For BDL, we anesthetized mice and after midline laparotomy we ligated the common bile duct twice with silk sutures and closed the abdomen. We performed the sham surgery similarly, except that the bile duct was not ligated. Mice were killed 3 weeks after BDL. For acute liver injury, mice were fed a control or an HC diet for 4 weeks, and then were killed 5 days after BDL or 24 hours after a single injection of CCl_4. All animals received humane care in compliance with the National Research Council's criteria outlined in the "Guide for the Care and Use of Laboratory Animals," prepared by the US National Academy of Sciences and published by the US National Institutes of Health (Bethesda, MD).

Biochemical and Histologic Analysis

Serum concentrations of ALT, TGs, glucose, and cholesterol were determined as previously described. Hepatic TG content and liver hydroxyproline concentrations were measured as previously described.[1] Liver cholesterol levels or the cholesterol content of HSCs or Kupffer cells were measured using the Cholesterol/Cholesteryl Ester Quantitation Kit (BioVision, Mountain View, CA), following the manufacturer's instructions. We detemined the cholesterol content of HSCs or Kupffer cells immediately after isolation. Liver tissues were fixed in 4% paraformaldehyde, embedded in paraffin, and stained with H&E and a Masson trichrome solution. For protein or RNA analysis, tissues were frozen in liquid nitrogen and stored at −80°C until needed.

Kupffer Cell Depletion

We injected dichloromethylene diphosphonic acid (clodronate)-loaded or phosphate-buffered saline–loaded liposomes (Encapsula NanoSciences, Nashville, TN) intravenously into mice (200 μL per mouse).

HSC Isolation and Culture

HSCs were isolated from mice or rats as previously described.[1] We cultured HSCs on uncoated plastic tissue culture dishes in Dulbecco's modified Eagle medium containing 1% or 10% fetal bovine serum, and used them as nonpassaged primary cultures only. For FC accmulation in HSCs, primary HSCs were incubated with AcLDL (50 μg/mL) plus compound 58035 (10 μg/mL) for 16 hours. We used enzyme-linked immunosorbent assay kits for mouse monocyte chemoattractant protein-1 (Thermo Scientific, Rodkford, IL) or macrophage inflammatory protein-2 (R&D Systems) for quantification of secreted monocyte chemoattractant protein-1 and macrophage inflammatory protein-2 in HSC cultures.

Kupffer Cell Isolation and Culture

Kupffer cells were isolated from mice, and cultured as previously described.[2]

Immunohistochemistry

Paraffinized sections were deparaffinized, rehydrated, blocked with normal horse serum, and incubated with anti-αSMA monoclonal antibody 1A4 (Dako Japan, Kyoto, Japan), anti-F4/80 monoclonal antibody (Serotec, Oxford, UK), or anti-CD3 monoclonal antibody (Abcam, Cambridge, UK) overnight at 4°C. The mouse F4/80 antigen is a 160-kilodalton glycoprotein expressed by mouse macrophages; antimouse F4/80 antibody binds mouse monocytes/macrophages and Kupffer cells. The antigen is not expressed by either lymphocytes or polymorphonuclear cells. Antibody binding was detected by incubation with biotinylated antimouse immunoglobulin G antibody and visualized with a Vectastain Elite ABC Kit (Vector Laboratories, Inc, Burlingame, CA) by reaction with Vectastatin DAB Substrate (Vector).

Fresh-frozen liver sections were cut 6-mm thick on a cryostat, collected on slides, and immediately dried. The sections were fixed with acetone. The slides were incubated overnight with anti-CD68 Ab (Serotec), followed by incubation with Histofine Simple Stain Mouse MAX-PO (Nichirei, Tokyo, Japan) for 1 hour.

Neutrophil Infiltration

Neutrophils in the liver were stained using the naphthol AS-D chloroacetate esterase technique. Paraffin-embedded liver sections were stained using the naphthol AS-D chloroacetate kit (Sigma Chemical Co, St. Louis, MO) following the manufacturer's instructions.

Detection of Apoptosis

Terminal deoxynucleotidyl transferase–mediated deoxyuridine nick-end labeling staining (Chemicon International, Temecula, CA) was performed on specimens to assess apoptosis. Apoptosis was quantified by counting positively stained cells in 10 random fields at 200× magnification. Apoptosis was measured for each specimen as a percentage of total cells per field. Antibody binding was detected by incubation with biotinylated anti-mouse immunoglobulin G antibody and visualized with a Vectastain Elite ABC Kit (Vector Laboratories, Inc) by reaction with Vectastatin DAB Substrate (Vector).

Mitochondrial Isolation and Characterization

A mitochondrial fraction was enriched from 100-mg liver specimens with the Mitochondria Isolation Kit (Sigma) by 2 consecutive centrifugation steps at 600 g and 11,000 g. The electrochemical proton gradient ($\Delta\Psi$) of the inner mitochondrial membrane was tested by measuring the uptake of the fluorescent carbocyanine dye JC-1 (Sigma) into mitochondria, as specified by the manufacturer.[1] Relative $\Delta\Psi$ was calculated in comparison with values obtained in control-diet–fed mice.

Real-Time Quantitative and Reverse-Transcription Polymerase Chain Reaction Analysis

Total RNA was extracted from total liver homogenates or HSCs using TaKaRa RNAiso Reagent (TaKaRa Bio, Ohtsu, Japan), according to the manufacturer's instructions. Reverse transcription was performed as previously described.[1] For quantitation of mRNA expression, the following real-time polymerase chain reaction amplifications were performed in duplicate, using the SYBR Premix Ex Taq (Perfect Real Time) kit (TaKaRa Bio) in a Thermal Cycler Dice Real Time system (TaKaRa Bio).

Western Blot Analysis

Preparation of whole-cell protein extracts from HSCs, electrophoresis of whole-cell protein extracts (5 μg), and subsequent blotting were performed using antibodies against TLR4 and β-actin, as previously described.[1]

Flow Cytometry Analysis

HSC surface expression of TLR4 was detected by flow cytometry of live cells stained with phycoerythrin-conjugated anti-TLR4 antibody (Abcam) or phycoerythrin-conjugated anti-immunoglobulin G isotype control. A total of 10,000 cells/condition were analyzed in a FACScan, using the FACSCalibur (Becton Dickinson, Franklin Lakes, NJ).

Isolation of Late Endosomes/Lysosomes From HSCs

Late endosomal/lysosomal fractions were prepared from HSCs using the lysosome isolation kit (Sigma) following the manufacturer's instructions.

References

1. Tomita K, Tamiya G, Ando S, et al. Tumour necrosis factor alpha signalling through activation of Kupffer cells plays an essential role in liver fibrosis of non-alcoholic steatohepatitis in mice. Gut 2006; 55:415–424.
2. Tomita K, Azuma T, Kitamura N, et al. Leptin deficiency enhances sensitivity of rats to alcoholic steatohepatitis through suppression of metallothionein. Am J Physiol Gastrointest Liver Physiol 2004; 284:G1078–G1085.
3. Paik YH, Schwabe RF, Bataller R, et al. Toll-like receptor 4 mediates inflammatory signaling by bacterial lipopolysaccharide in human hepatic stellate cells. Hepatology 2003;37:1043–1055.
4. Seki E, De Minicis S, Osterreicher CH, et al. TLR4 enhances TGF-beta signaling and hepatic fibrosis. Nat Med 2007;13:1324–1332.

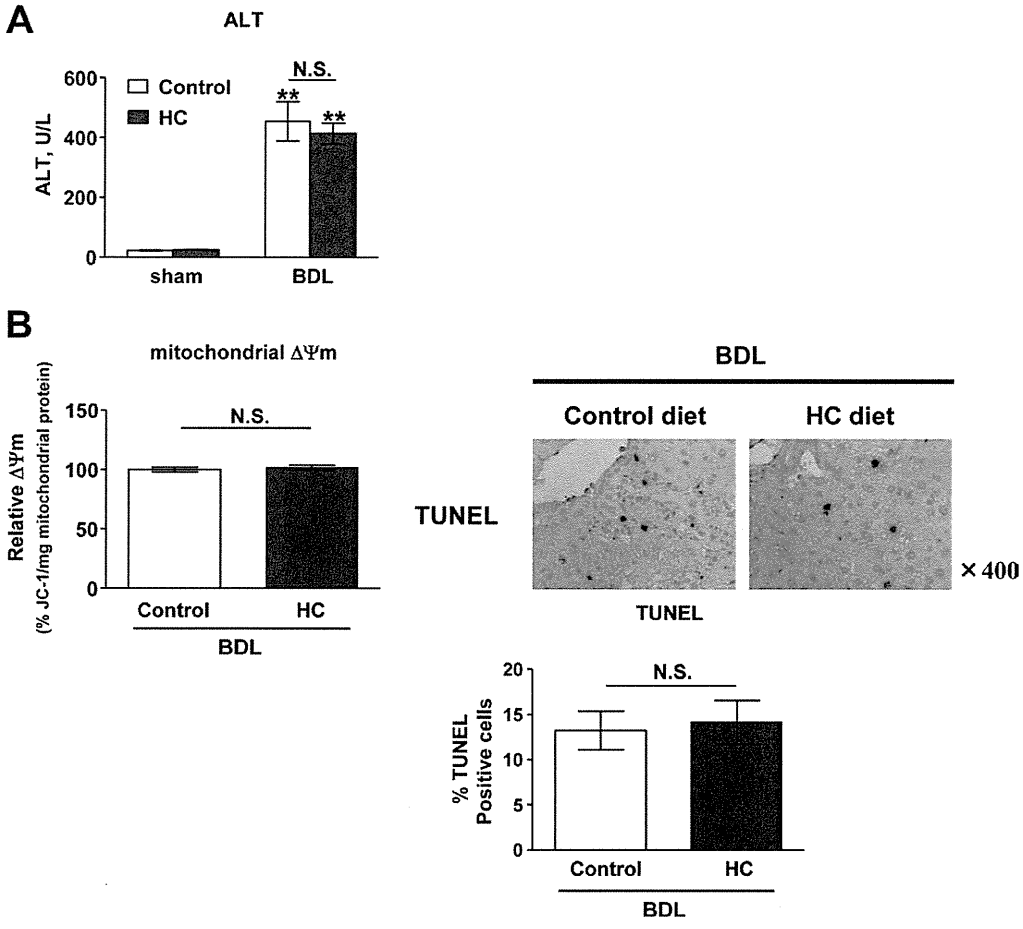

Supplementary Figure 1. Effects of the HC diet on acute liver injury induced by BDL treatment. After being fed a control or an HC diet for 4 weeks, C57BL/6 mice were subjected to acute liver injury, induced 5 days after BDL treatment (N = 5/group). (*A*) Serum ALT activities (N = 5/group). (*B*, *left panels*) Electrochemical proton gradient of the inner mitochondrial membrane (N = 5/group). The calculated relative $\Delta\Psi$ was normalized to the values obtained in mice from the control diet–BDL group. (*B*, *right panels*) The percentage of terminal deoxynucleotidyl transferase–mediated deoxyuridine nick-end labeling (TUNEL)-positive hepatocytes (N = 5/group) and the representative sections.

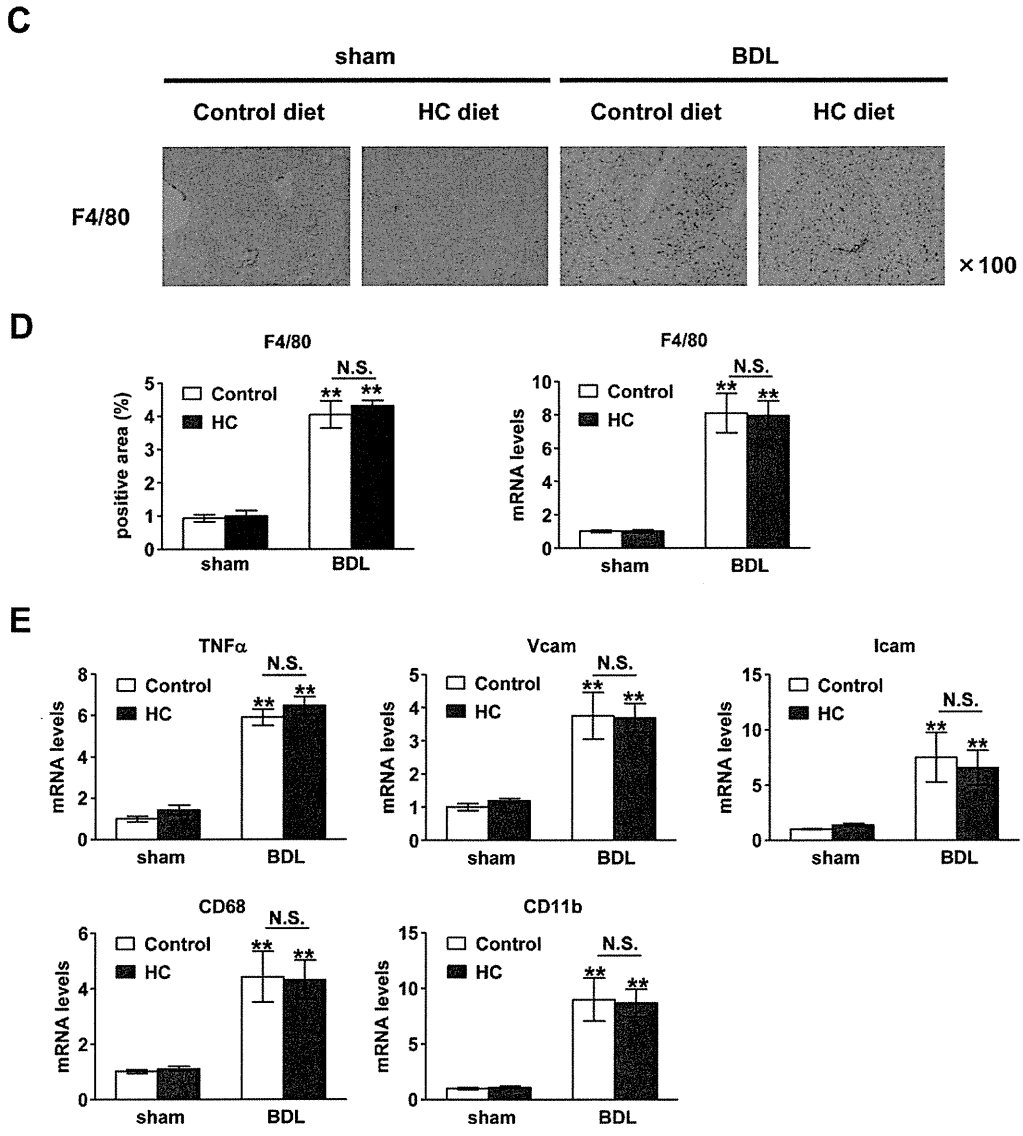

Supplementary Figure 1 (Cont'd.). (*C*) Immunohistochemical detection of F4/80-positive cells in livers. (*D*) Quantification of F4/80 by immunohistochemical staining and mRNA levels. (*E*) Hepatic expression of TNFα, vascular cell adhesion molecule-1 (VCAM-1), intercellular adhesion molecule-1 (ICAM-1), CD68, and CD11b mRNA (N = 5/group). $^{**}P < .01$ compared with control diet–sham-operated group.

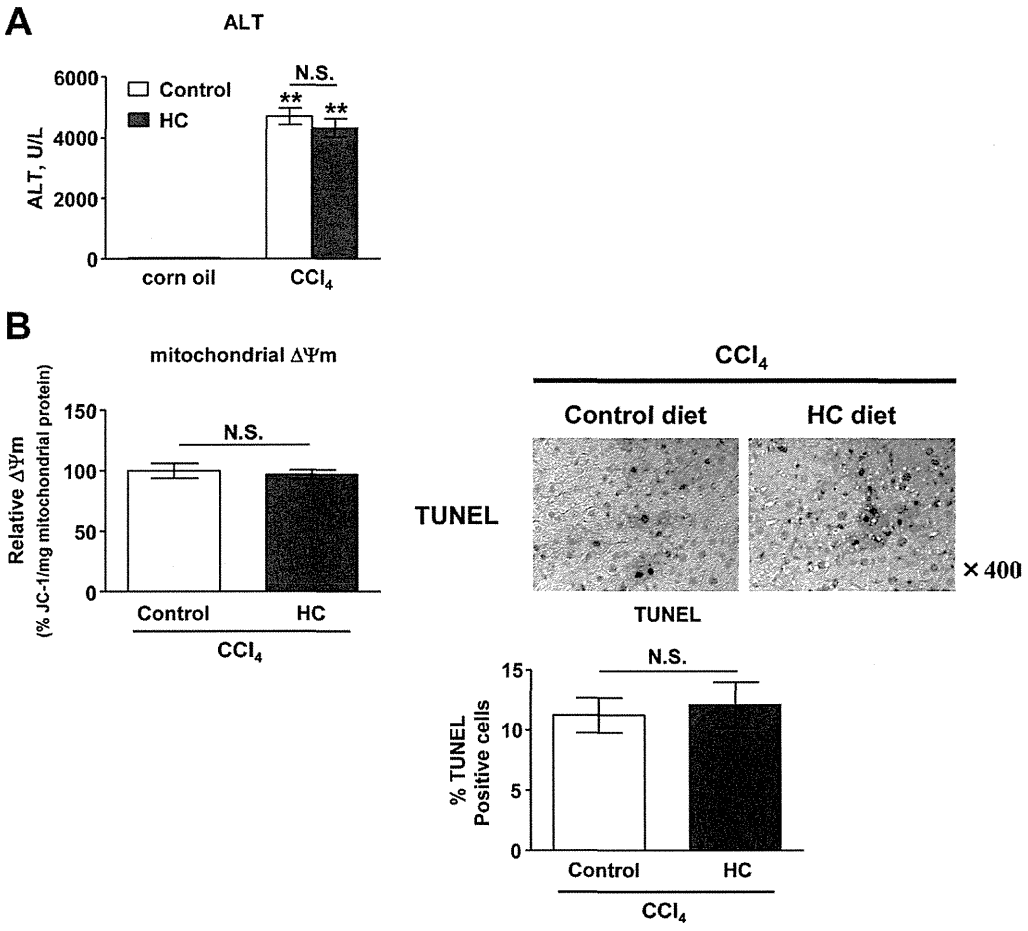

Supplementary Figure 2. Effects of the HC diet on acute liver injury induced by CCl_4 treatment. After being fed a control or an HC diet for 4 weeks, C57BL/6 mice were subjected to acute liver injury induced by a single injection of CCl_4 (N = 5/group). (*A*) Serum ALT activities (N = 5/group). (*B*, *left panels*) Electrochemical proton gradient of the inner mitochondrial membrane (N = 5/group). The calculated relative $\Delta\Psi$ was normalized to the values obtained in mice from the control diet–CCl_4 group. (*B*, *right panels*) The percentage of terminal deoxynucleotidyl transferase–mediated deoxyuridine nick-end labeling (TUNEL)-positive hepatocytes (N = 5/group) and the representative sections.

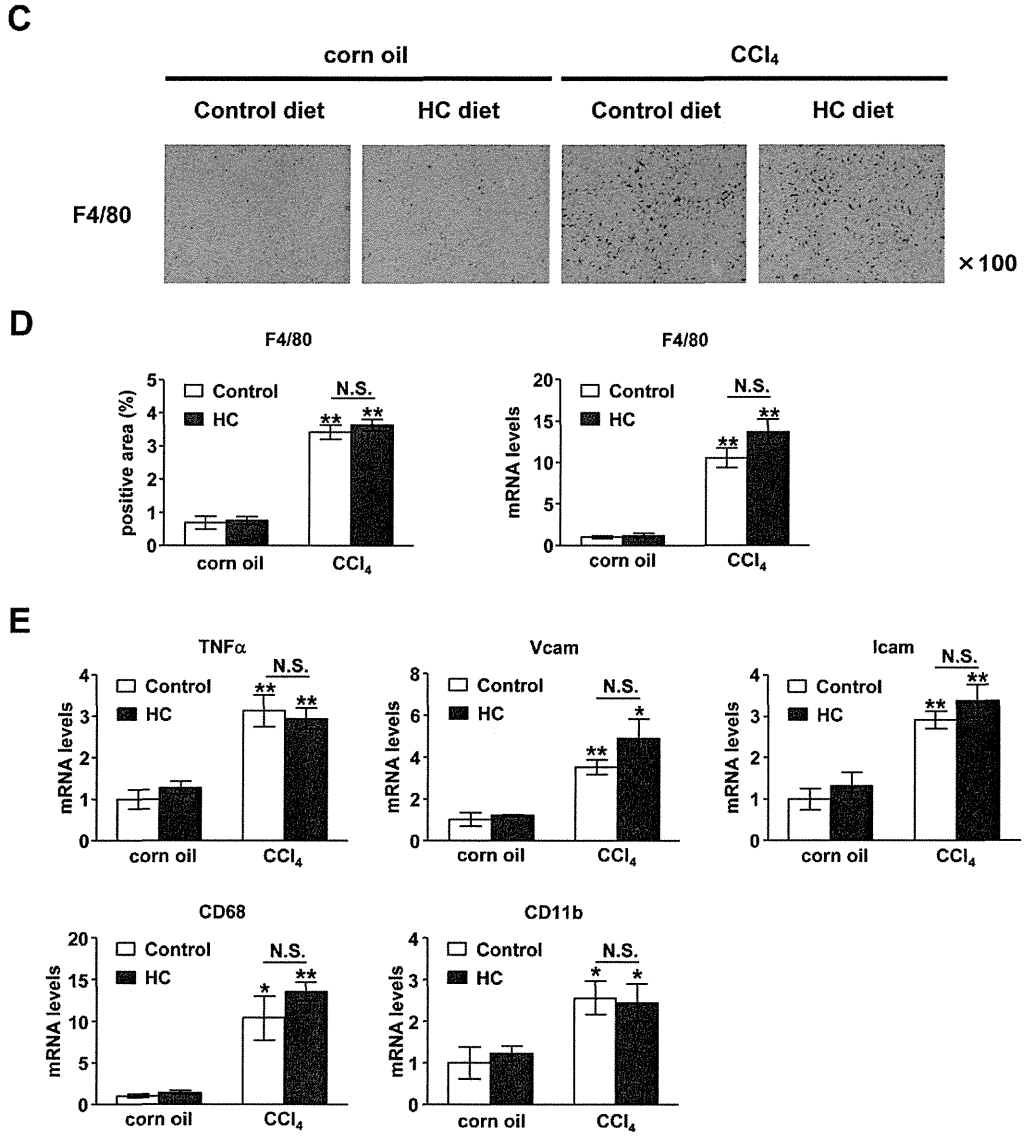

Supplementary Figure 2 (Cont'd.). (*C*) Immunohistochemical detection of F4/80-positive cells in livers. (*D*) Quantification of F4/80 by immunohistochemical staining and mRNA levels. (*E*) Hepatic expression of TNFα, vascular cell adhesion molecule-1 (VCAM-1), intercellular adhesion molecule-1 (ICAM-1), CD68, and CD11b mRNA (N = 5/group). *$P < .05$ and **$P < .01$ compared with control diet–corn oil group.

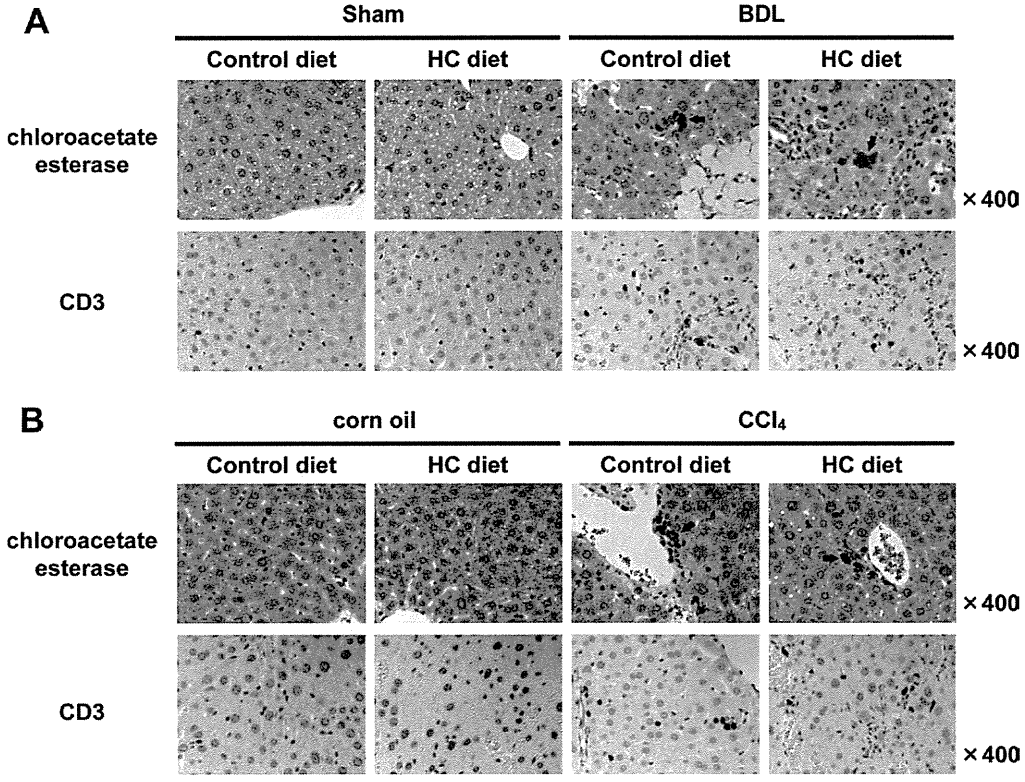

Supplementary Figure 3. Effects of the HC diet on the BDL- or CCl_4-mediated infiltration of T cells and neutrophils into the liver. After being fed a control or an HC diet for 4 weeks, C57BL/6 mice were subjected to (*A*) 3-week BDL or (*B*) CCl_4 treatment twice a week for 4 weeks to induce liver fibrosis (N = 5–7/group). (*Upper panels*) Staining by the naphtol AS-D chloroacetate esterase technique for detection of neutrophils and (*lower panels*) immunohistochemical staining for CD3 for detection of T cells.

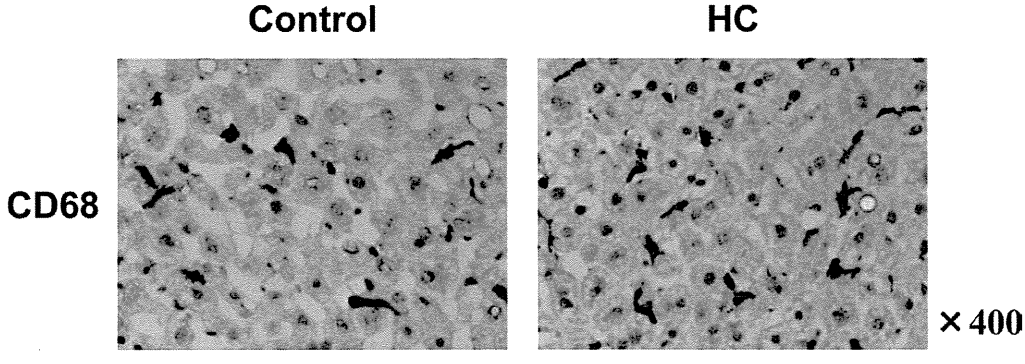

Supplementary Figure 4. HC diet did not induce the formation of hepatic macrophage foam cells. Immunohistochemical detection of CD68-positive cells in livers: mice fed a control diet (*left panel*) or an HC diet (*right panel*) for 8 weeks.